ChemComm

COMMUNICATION

View Article Online
View Journal

Cite this: DOI: 10.1039/c7cc03497k

Received 5th May 2017,
Accepted 4th July 2017

DOI: 10.1039/c7cc03497k

rsc.li/chemcomm

Highly effective molecule converting strategy based on enzyme-free dual recycling amplification for ultrasensitive electrochemical detection of ATP†

Hua Xie, Yaqin Chai, Yali Yuan* and Ruo Yuan *

An enzyme-free and highly effective molecule converting strategy based on target-driven catalytic hairpin assembly and Mg^{2+}-dependent DNAzyme recycling dual-amplification was proposed to construct an ultrasensitive electrochemical biosensor for adenosine triphosphate (ATP) detection.

The translation of a target molecule to DNA detection has been proved to be a fascinating method for sensitive assay owing to the fact that it allows combination with many DNA-based amplification strategies, such as rolling circle amplification,[1–3] loop-mediated isothermal amplification,[4,5] ligase chain reaction,[6] isothermal exponential amplification reaction[7–9] and enzyme cleavage recycling.[10–14] Overall, most of the reported works are highly enzyme-dependent, in which at least one type of protein enzyme is essential to catalyze the DNA amplification process. As we know, protein enzyme possesses the drawbacks of exorbitant cost as well as inherent instability,[15,16] which may affect the DNA amplification efficiency with a limited target molecule conversion ratio. Meanwhile, the enzymatic amplification process can easily produce a "false-positive" result.[17] Accordingly, it is particularly valuable to develop a highly efficient molecule converting strategy without the participation of any protein enzymes for sensitive detection of target molecules.

Recently, enzyme-free DNA recycling amplification[18–20] has attracted much attention due to the advantages of simplicity and low cost. Tang's group developed an enzyme-free strategy to detect proteins on the basis of catalytic hairpin assembly (CHA).[21] Chen's group realized a protein assay based on an enzyme-free strand displacement reaction for signal amplification.[22] Despite the success in constructing enzyme-free target molecular converting strategies, these methods commonly involved utilizing just a single DNA recycling amplification technique for generating output DNA, in which the target conversion ratio was limited to some extent. The detection sensitivities achieved were thus still not competitive to meet the demands of practical applications. If one input target initially induces the first cycle reaction for generating a few product DNA, which subsequently serve as triggers to induce another non-enzymatic cycle reaction to yield massive output DNA, it might greatly enhance the target conversion ratio, holding a potential to construct a sensitive electrochemical biosensor for target molecule detection.

Herein, aiming at improving the analytical performance and simplifying the operation procedures for biosensors, an enzyme-free and highly effective molecule converting strategy by using target-driven CHA and Mg^{2+}-dependent DNAzyme[23–25] recycling dual-amplification was described and successfully applied in an electrochemical biosensor for ultrasensitive electrochemical detection of adenosine triphosphate (ATP). Briefly, the binding of two split aptamers toward ATP initiated CHA to perform the first recycling amplification and convert input ATP into enzymatic sequences (termed as HP1–HP2), which could subsequently hybridize with substrate hairpins HP3 on magnetic polystyrene microspheres (PSC) to form Mg^{2+}-dependent DNAzymes. Therefore, the presence of Mg^{2+} caused the second recycling cleavage of HP3 to generate output DNA S1, realizing the conversion of one input ATP into massive output DNA S1 with a dramatically enhanced conversion ratio. Through a ternary "Y" junction structure, the released DNA S1 could hybridize with DNA1 and methylene blue labeled DNA2 (DNA2-MB) to produce a noticeable electrochemical signal. Compared with other strategies, the developed method avoided the anticipation of any protein enzymes and realized the dual-amplification, making the system sensitive. Moreover, the redox probe MB approached the electrode effectively reducing their inter-distance with a rather higher electrochemical signal for sensitivity improvement. The strategy described here might open a new avenue for developing nonenzymatic dual DNA recycling amplification with a high target molecular converting efficiency to sensitively detect the targets.

The principle of the electrochemical biosensor on the basis of ATP translation and detection is illustrated in Scheme 1. The ATP

Key Laboratory of Luminescent and Real-Time Analytical Chemistry (Southwest University), Ministry of Education, College of Chemistry and Chemical Engineering, Southwest University, Chongqing 400715, P. R. China.
E-mail: y198688@swu.edu.cn, yuanruo@swu.edu.cn; Fax: +86-23-68253172; Tel: +86-23-68252277

† Electronic supplementary information (ESI) available: Experimental details and electrochemical characterization. See DOI: 10.1039/c7cc03497k

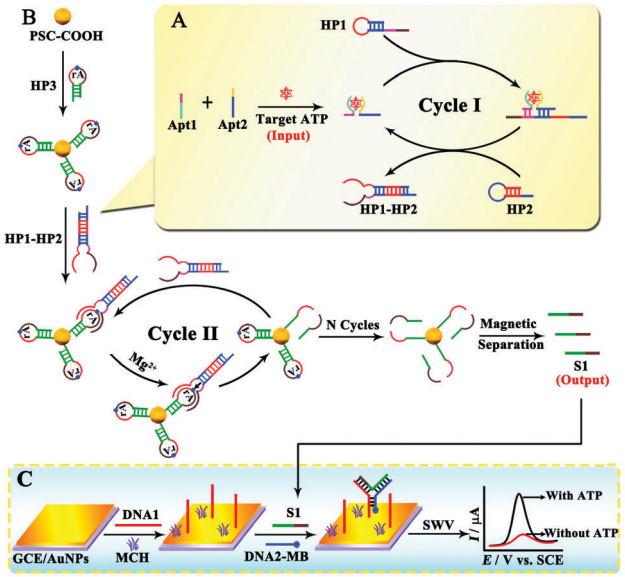

Scheme 1 Schematic illustration of the electrochemical biosensor for ATP detection on the basis of a highly effective molecule converting strategy: (A) the ATP-driven CHA process, (B) Mg^{2+}-dependent DNAzyme cleavage recycling amplification process, and (C) the assembly of the electrode and electrochemical detection of ATP.

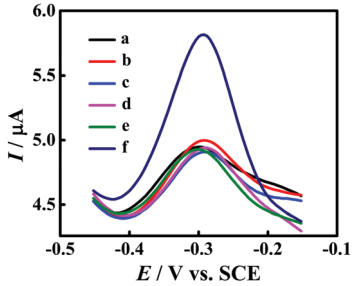

Fig. 1 Typical SWV responses of the proposed electrochemical biosensor toward the analysis of 0 (a) and 10 nM (f) ATP. The curves correspond to the different experimental conditions performed at no Apt1 (b), no Apt2 (c), no HP1 (d) and no HP2 (e), respectively. SWV measurements were carried out by scanning the potential from −0.45 V to −0.15 V in phosphate buffered solution (PBS) (pH 7.0, 0.1 M) with a pulse amplitude of 25 mV, a step potential of 4 mV and a frequency of 25 Hz.

conversion process consisted of ATP-driven CHA and Mg^{2+}-dependent DNAzyme cleavage recycling amplification. In the presence of target ATP, Apt1 and Apt2 containing split ATP aptamer subunits could co-recognize ATP to form an Apt1–ATP–Apt2 structure, which could hybridize with HP1 based on the toehold-mediated strand displacement reaction. The newly exposed region within HP1 could further hybridize with HP2 through toehold-mediated DNA strand displacement again, accompanied by the release of the Apt1–ATP–Apt2 structure. The liberated Apt1–ATP–Apt2 structure participated in the next hybridization and strand displacement process (Cycle I), resulting in the generation of numerous HP1–HP2 hybridized complexes. Afterwards, the formed HP1–HP2 hybrid could specifically bind to the substrate strand HP3 which was immobilized on the PSC-COOH through complementary base pairing, forming an active Mg^{2+}-dependent DNAzyme structure. In the presence of Mg^{2+}, HP3 was autocatalytically cleaved, in which the HP1–HP2 duplex was liberated and initiated another cleavage reaction in adjacent locations, accompanied by the production of massive output DNA S1 (Cycle II). Benefiting from dual cyclic amplification, each input target ATP was converted into more than one output S1. After magnetic separation, S1 was captured by DNA1 assembled on the electrode to form a "Y" junction structure with the aid of DNA2-MB. Owing to the fact that MB approached the electrode, these formed "Y" junction structures were thus expected to detect a low level of ATP with high sensitivity.

The feasibility of our proposed protocol for ATP detection was verified by comparing the square wave voltammetry (SWV) responses resulting from different biosensors. As depicted in Fig. 1, small SWV response currents were observed in the absence of target ATP (curve a), Apt1 (curve b) or Apt2 (curve c), which were attributed to the fact that there was no Apt1–ATP–Apt2 structure. Similarly, in the absence of HP1 (curve d) or HP2 (curve e), the Apt1–ATP–Apt2 structure was formed, however subsequent CHA and Mg^{2+}-dependent DNAzyme cleavage processes were inhibited, which caused negligible current changes. In contrast, in the presence of target ATP, a conspicuous enhanced current response (curve f) was obtained due to the assembling of the "Y" junction structures on the electrode through CHA and Mg^{2+}-dependent DNAzyme cleavage processes which were ascribed to the simultaneous recognition of Apt1 and Apt2 toward target ATP. These results indicated the great potential of the developed biosensor for enzyme-free sensitive ATP determination.

The electrodeposition time was not only related to the morphology of AuNPs, but also had a significant influence on the electrochemical performance. Therefore, scanning electron microscopy (SEM) was first applied to characterize the morphologies of AuNPs. From Fig. 2A we could see that AuNPs possessed different morphologies at different electrodeposition times. Moreover, after electrodepositing a layer of AuNPs at different electrodeposition times on a bare glassy carbon electrode, we also investigated the cyclic voltammetry (CV) response of AuNPs in a 5.0 mM $[Fe(CN)_6]^{3-/4-}$ solution containing 0.1 M KCl. As shown in Fig. 2B, the current increased accompanied with the increase of the electrodeposition time and reached the maximum at 30 s. However, when the electrodeposition time was more than 30 s, the current decreased. This might be due to the fact that an overdense AuNP film on the electrode surface can obstruct the electron transfer. Thus, 30 s was chosen as the optimized electrodeposition time to construct the electrochemical biosensor.

The electrochemical signal derived from MB of the "Y" junction structure which was related to the amount of S1, so, the cleavage time of Mg^{2+}-dependent DNAzyme and the formation time of the "Y" junction structure were optimized for the detection of ATP (10 nM) (the ATP detection process is shown in the ESI†). As displayed in Fig. 2C, the current response successively increased with the augment of the incubation time up to 60 min. Once the incubation time exceeded 60 min, there was no obvious change in current. Therefore, 60 min was selected as the optimal cleavage time for Mg^{2+}-dependent

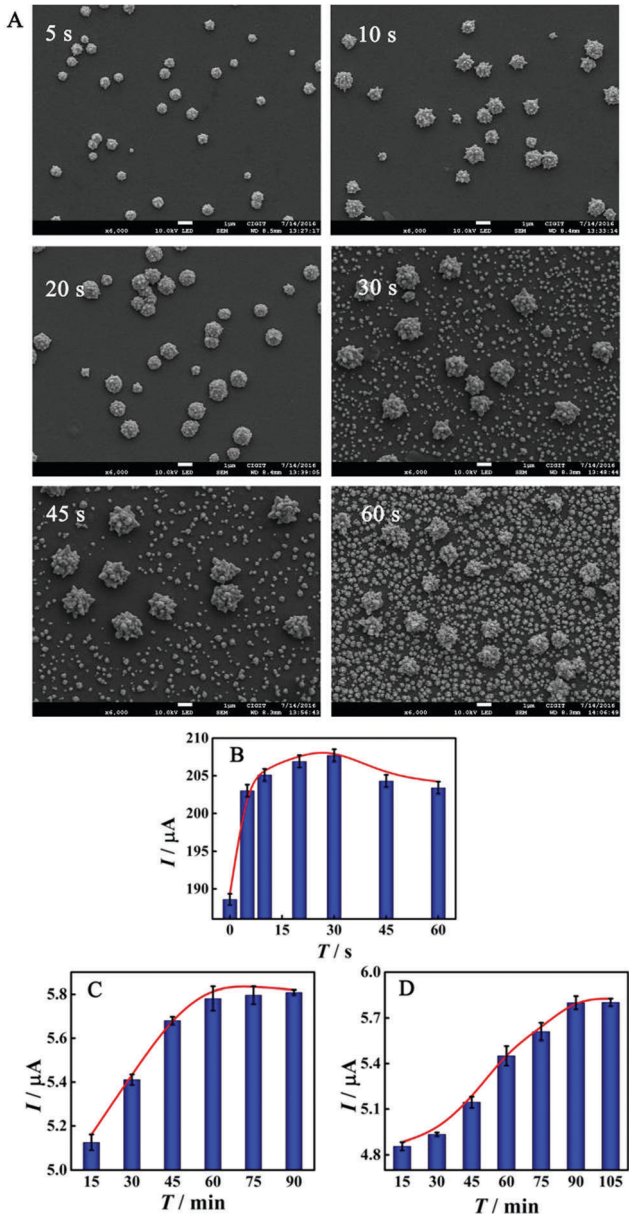

Fig. 2 (A) The SEM images of different electrodeposition times of AuNPs. The scale bar corresponds to 1 μm. (B) The corresponding CV responses of different electrodeposition times of AuNPs in 5.0 mM $[Fe(CN)_6]^{3-/4-}$ solution containing 0.1 M KCl. Effects of (C) Mg^{2+}-dependent DNAzyme cleavage time and (D) the formation time of the "Y" junction structure on the SWV responses of the biosensor in the presence of ATP (10 nM). Error bars, SD, n = 3. Other conditions are as shown in Fig. 1.

DNAzyme. As illustrated in Fig. 2D, it was obvious that with the increase of incubation time, a consecutive increase in current was observed in the range of 15–90 min, while further increasing the time did not lead to appreciable changes in current, indicating that 90 min was sufficient for the formation of the "Y" junction structure. Thus, an optimized incubation time of 90 min was adopted throughout the experiments.

To investigate the sensitivity of the proposed electrochemical biosensor, various concentrations of ATP were incubated and the corresponding SWV signals were recorded under the optimal

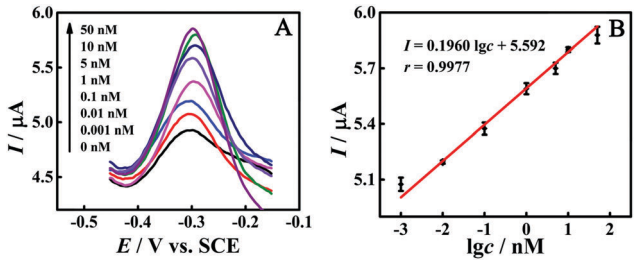

Fig. 3 (A) SWV responses of an electrochemical biosensor toward 0 nM, 0.001 nM, 0.01 nM, 0.1 nM, 1 nM, 5 nM, 10 nM and 50 nM of ATP. (B) The corresponding calibration plot between the peak current and the logarithm of ATP concentration. Error bars, SD, n = 3. Other conditions are as shown in Fig. 1.

conditions. As depicted in Fig. 3A, it was apparent that when the concentration of ATP was varied from 0 nM to 50 nM, a gradual increase in the SWV peak currents was observed. Fig. 3B shows the corresponding calibration plot between the peak current and the logarithm of the concentration of ATP, in which the peak current was linearly dependent on the logarithm of ATP concentration ranging from 0.001 nM to 50 nM. The linear regression equation could be expressed as $I = 0.1960 \lg c + 5.592$ with a correlation coefficient of 0.9977. Moreover, the detection limit was estimated to be 0.45 pM according to the signal-to-noise ratio of three, which was lower than those of the recently reported works shown in Table S2 (see the ESI†).

Selectivity is a key factor for evaluating the performance of developed electrochemical biosensor. Therefore, CTP, GTP and UTP were chosen as the interference substrates to study the specificity. As can be seen from Fig. 4, there was no significant change in the SWV current response in the detection of 100 nM GTP, 100 nM CTP, and 100 nM UTP in comparison with the blank test. In contrast, a high SWV current response was observed when the electrochemical biosensor was incubated with ATP (10 nM). In addition, the presence of a mixture containing 100 nM GTP, 100 nM CTP, 100 nM UTP and 10 nM ATP did not lead to a significant signal change compared with 10 nM ATP. These results indicated that the fabricated biosensor had excellent selectivity.

The reproducibility was investigated with four electrodes toward the same concentration of ATP (10 nM) (termed as intra-assay) and the same electrode repeated for four measurements (termed as

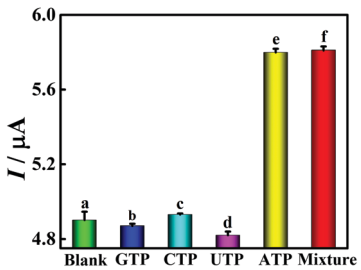

Fig. 4 The specificity of our protocol toward (a) 0 nM ATP, (b) 100 nM GTP, (c) 100 nM CTP, (d) 100 nM UTP, (e) 10 nM ATP, and (f) a mixture containing 100 nM GTP, 100 nM CTP, 100 nM UTP and 10 nM ATP. Error bars, SD, n = 3. Other conditions are as shown in Fig. 1.

inter-assay). The relative standard deviation (RSD) values of the inter-assay and the intra-assay were 4.5% and 3.4%, respectively, which revealed an acceptable reproducibility of our protocol.

To assess the practical application of the constructed electrochemical biosensor, a recovery experiment was performed with the standard addition method. Different concentrations of ATP (0.01 nM, 0.1 nM, 1 nM and 10 nM) were spiked into 100-diluted human serum samples (obtained from 9th People's Hospital of Chongqing), followed by detection of ATP with the proposed electrochemical biosensor. It was found from Table S3 (see the ESI†) that recovery was in the range of 92.6–104% and the RSD value was between 2.4% and 6.1%, which indicated that the proposed electrochemical biosensor could be applied to monitor ATP in human serum.

In conclusion, we proposed an enzyme-free and highly effective small molecule converting strategy for the ultrasensitive electrochemical detection of ATP on the basis of target-driven catalytic hairpin assembly and Mg^{2+}-dependent DNAzyme recycling dual-amplification. During this process, one input target ATP could be converted into massive output DNA S1, thus enhancing the conversion ratio as well as improving the detection sensitivity. Moreover, the overall sensing strategy was enzyme-free, which also avoided the drawbacks of complicated operation procedures and special reaction conditions. Due to the advantages of high sensitivity and excellent selectivity, the detection system demonstrated here could be conveniently extended to detect other analytes by changing two aptamers with corresponding recognition domains.

This work was financially supported by the NNSF of China (21505107, 21575116, 21675129), Chongqing Research Program of Basic Research and Frontier Technology (cstc2016jcyjA0189), and the Fundamental Research Funds for the Central Universities (SWU115037).

Notes and references

1 B. Q. Liu, B. Zhang, G. N. Chen, H. H. Yang and D. P. Tang, *Anal. Chem.*, 2014, **86**, 7773–7781.
2 Y. S. Huang, W. L. Xu, G. Y. Liu and L. L. Tian, *Chem. Commun.*, 2017, **53**, 3038–3041.
3 Y. S. Guo, Y. J. Wang, S. Li, L. Niu, D. Wei and S. S. Zhang, *Chem. Commun.*, 2017, **53**, 4826–4829.
4 Y. Hu, P. Xu, J. Luo, H. X. He and W. B. Du, *Anal. Chem.*, 2017, **89**, 745–750.
5 C. S. Ball, Y. K. Light, C. Y. Koh, S. S. Wheeler, L. L. Coffey and R. J. Meagher, *Anal. Chem.*, 2016, **88**, 3562–3568.
6 J. B. Chen, B. Deng, P. Wu, F. Li, X. F. Li, X. C. Le, H. Q. Zhang and X. D. Hou, *Chem. Commun.*, 2016, **52**, 1816–1819.
7 Y. Huang, H. Li, Y. Y. Zhang, W. W. Li, L. Z. Sun and G. X. Li, *Chem. Commun.*, 2015, **51**, 11004–11007.
8 H. Z. Wang, Y. Wang, S. Liu, J. H. Yu, W. Xu, Y. N. Guo and J. D. Huang, *Chem. Commun.*, 2015, **51**, 8377–8380.
9 Q. W. Xue, L. Wang and W. Jiang, *Chem. Commun.*, 2015, **51**, 13538–13541.
10 Y. F. Qin, L. L. Zhang, S. T. Li, J. J. Zhao, Y. Huang, S. L. Zhao and Y. M. Liu, *Chem. Commun.*, 2017, **53**, 455–458.
11 Y. Tan, X. F. Wei, Y. Zhang, P. L. Wang, B. Qiu, L. H. Guo, Z. Y. Lin and H. H. Yang, *Anal. Chem.*, 2015, **87**, 11826–11831.
12 L. Ge, W. X. Wang, X. M. Sun, T. Hou and F. Li, *Anal. Chem.*, 2016, **88**, 2212–2219.
13 C. Y. Yang, B. T. Dou, J. M. Yang, R. Yuan and Y. Xiang, *Chem. Commun.*, 2016, **52**, 8707–8710.
14 Z. H. Yang, Y. Zhuo, R. Yuan and Y. Q. Chai, *Anal. Chem.*, 2016, **88**, 5189–5196.
15 D. P. Tang, B. L. Su, J. Tang, J. J. Ren and G. N. Chen, *Anal. Chem.*, 2010, **82**, 1527–1534.
16 W. J. Wang, J. J. Li, K. Rui, P. P. Gai, J. R. Zhang and J. J. Zhu, *Anal. Chem.*, 2015, **87**, 3019–3026.
17 F. Xuan, T. W. Fan and I. M. Hsing, *ACS Nano*, 2015, **9**, 5027–5033.
18 S. Bi, S. Z. Yue, Q. Wu and J. Y. Ye, *Chem. Commun.*, 2016, **52**, 5455–5458.
19 C. C. Chang, C. P. Chen, C. Y. Chen and C. W. Lin, *Chem. Commun.*, 2016, **52**, 4167–4170.
20 X. X. Li, S. J. Ye and X. L. Luo, *Chem. Commun.*, 2016, **52**, 10269–10272.
21 Y. N. Tang, Y. W. Lin, X. L. Yang, Z. X. Wang, X. C. Le and F. Li, *Anal. Chem.*, 2015, **87**, 8063–8066.
22 P. P. Chen, P. Wu, Y. X. Zhang, J. B. Chen, X. M. Jiang, C. B. Zheng and X. D. Hou, *Anal. Chem.*, 2016, **88**, 12386–12392.
23 L. M. Wei, X. Y. Wang, D. Wu, C. Li, Y. M. Yin and G. X. Li, *Chem. Commun.*, 2016, **52**, 5633–5636.
24 D. G. He, X. He, X. Yang and H. W. Li, *Chem. Sci.*, 2017, **8**, 2832–2840.
25 S. Lilienthal, M. Klein, R. Orbach, I. Willner, F. Remacle and R. D. Levine, *Chem. Sci.*, 2017, **8**, 2161–2168.

